Interconversion algorithm between mechanical and dielectric relaxation measurements for acetate of *cis*- and *trans*-2-phenyl-5-hydroxymethyl-1,3-dioxane

A. Garcia-Bernabé,[1,*] J. V. Lidón-Roger,[2,3] M. J. Sanchis,[1,4] R. Díaz-Calleja,[4] and L. F. del Castillo[5]

[1]*Departamento de Termodinámica Aplicada, Universitat Politècnica de València, 46022-Valencia, Spain*

[2]*Departamento de Ingeniería Electrónica, Universitat Politècnica de València, 46022-Valencia, Spain*

[3]*Centro de Reconocimiento Molecular y Desarrollo Tecnológico (IDM), Universitat Politècnica de València, 46022-Valencia, Spain*

[4]*Instituto de Tecnología Eléctrica, Avenida Juan de la Cierva 24, 46980 Paterna-Valencia, Spain*

[5]*Instituto de Investigaciones en Materiales, Universidad Nacional Autónoma de México, Ap. Postal 70-360, Coyoacán, México Distrito Federal 04510, Mexico*

(Received 16 February 2015; revised manuscript received 24 July 2015; published 12 October 2015)

The dielectric and mechanical spectroscopies of acetate of *cis*- and *trans*-2-phenyl-5-hydroxymethyl-1,3-dioxane are reported in the frequency domain from 10^{-2} to 10^{6} Hz. This ester has been selected in this study for its predominant α relaxation with regard to the β relaxation, which can be neglected. This study consists of determining an interconversion algorithm between dielectric and mechanical measurements, given by using a relation between rotational and translational complex viscosities. These important viscosities were obtained from measures of the dielectric complex permittivity and by dynamic mechanical analysis, respectively. The definitions of rotational and translational viscosities were evaluated by means of fractional calculus, by using the fit parameters of the Havriliak-Negami empirical model obtained in the dielectric and mechanical characterization of the α relaxation. This interconversion algorithm is a generalization of the break of the Stokes-Einstein-Debye relationship. It uses a power law with an exponent defined as the shape factor, which modifies the translational viscosity. Two others factors are introduced for the interconversion, a shift factor, which displaces the translational viscosity in the frequency domain, and a scale factor, which makes equal values of the two viscosities. In this paper, the shape factor has been identified as the relation between the slopes of the moduli of the complex viscosities at higher frequency. This is interpreted as the degree of kinetic coupling between the molecular rotation and translational movements. Alternatively, another interconversion algorithm has been expressed by means of dielectric and mechanical moduli.

DOI: 10.1103/PhysRevE.92.042307 PACS number(s): 61.20.Lc, 77.22.Ch, 83.60.Df

I. INTRODUCTION

A comparison between dielectric and mechanical measurements has been reported by several authors. The first model was given by Germant [1], and afterwards by Dimarzio and Bishop [2]. They generalized the Debye equation assuming that the viscosity is frequency dependent, and is a complex function [1,3]

$$\frac{\varepsilon^*(\omega)-\varepsilon_\infty}{\varepsilon_0-\varepsilon_\infty}=\frac{1}{1+Ai\omega\eta^*(\omega)}, \tag{1}$$

where ω is the angular frequency, ε_∞ is the unrelaxed permittivity, ε_0 is the relaxed permittivity, η^* is the complex viscosity, and

$$A=\frac{4\pi r^3}{k_BT}\left(\frac{\varepsilon_0+2}{\varepsilon_\infty+2}\right).$$

r is the radius of the rotating dipole particles and k_B is the Boltzmann constant.

The linear viscoelasticity theory relates the complex viscosity to the mechanical modulus (G^*), namely,

$$G^*(\omega)=i\omega\eta^*(\omega). \tag{2}$$

By a combination of Eqs. (1) and (2), DiMarzio and Bishop related $\varepsilon^*(\omega)$ with the microscopic properties in the Dimarzio-Bishop (DMB) equation [2]

$$\frac{\varepsilon^*(\omega)-\varepsilon_\infty}{\varepsilon_0-\varepsilon_\infty}=\frac{1}{1+AG^*(\omega)} \tag{3}$$

Díaz-Calleja *et al.* [4] compared the dielectric and mechanical friction of poly(cyclohexyl acrylate). They noted that the Fatuzzo-Mason model [5] gave slightly better agreement than the original DMB model, and they concluded that the dielectric friction is of less importance than the mechanical friction.

Zorn *et al.* [6] do not quantitatively confirm the DMB equation in the analysis of a series of polybutadienes. The authors say that the DMB equation always predicts a narrower loss peak than is observed in the dielectric data. Several reasons have been given for this difference between the dielectric data and the DMB equation: (1) there is no distribution in the effective sphere radii, (2) neither an electrical nor a mechanical coupling of the individual dipoles is included, and (3) there is no anisotropy if the dipolar units or their local environment are taken into account.

Ferri and Castellani [7] used the DMB equation to compare dielectric and mechanical measurements of styrene-based copolymers. These authors concluded that these measurements are sensitive to different time and length scales, and that there is a scaling property of the mechanical and dielectric segmental relaxation processes.

Niss, Jakobsen, and Olsen [8] tested and reformulated the DMB equation for several glass-forming liquids. They relate the induced polarizability to the refractive index through

*agarciab@ter.upv.es

the Clausius-Mossotti approximation, that is, $\varepsilon_\infty = n^2$. This reformulated DMB equation does not diverge to infinity at high frequency. Therefore, a comparison of the reformulated DMB equation is qualitative and predicts a number of relations between shear and dielectric relaxation spectra. The authors suggest that the DMB model is a simplified one, but somewhat describes the relation between the dielectric permittivity and shear moduli.

Christensen and Olsen [9] proposed a different formulation of the DMB equation in terms of the dielectric modulus G_e^*, which is the inverse of the dielectric susceptibility. The proposed comparison of these authors uses the equality of the normalized dielectric (G_e^*) and mechanical (G_s^*) moduli. These normalized moduli are identical in shape, but with different loss peak frequencies. The authors found that the separation between the peak frequency of G_s^* and that of G_e^* is independent of temperature.

The plan of this paper is as follows: (1) The α relaxations of dielectric and mechanical measurements for the acetate of *cis*- and *trans*-2-phenyl-5-hydroxymethyl-1,3-dioxane (PHMD) have been characterized by means of the Havriliak-Negami (HN) equations for PHMD, where α relaxation is predominant and the secondary relaxations may be negligible. (2) The definition of dynamic rotational and translational viscosities has also been revised. (3) The interconversion algorithm for dynamic viscosities has been defined and used for PHMD. (4) A rotational modulus has been defined by means of the fractional time derivate for non-Newtonian behavior. (5) The interconversion algorithm has been defined in terms of rotational and shear moduli.

II. GENERAL BACKGROUND

Previous to this paper, we made a contribution for interconversion between mechanical and dielectric measurements using the definitions of rotational and translational viscosities [10]. The redefinition of the rotational and translational viscosities was done using fractional calculus. These two viscosities are related to a fractional Stokes-Einstein-Debye (FSED) equation. The interconversion was done using the Havriliak-Negami empirical model for α relaxation characterization. Then the interconversion between dielectric and mechanical measurements was formulated in terms of a power law relation between those viscosities with three interconversion parameters, namely, a scale factor (B), a shape factor (ξ), and a shift factor (δ):

$$\eta^*_{\mathrm{rot}}(\omega) = B[\eta^*_{\mathrm{trans}}(\omega\delta)]^{\xi}. \tag{4}$$

This relation between viscosities is a dynamic generalization of the Stokes-Einstein-Debye (SED) equation. In fact, the SED equation is based on the diffusion of a tracer particle which is dependent on the shear viscosity. This equality is adequate for spherical particles of any radius rotating in a Newtonian fluid. However, for dipoles of the same size as the molecular fluid particles in a viscoelastic fluid, as in the case of a supercooled liquid under nonergodic conditions, the SED relation breaks down. This effect has been recognized as the decoupling of translational diffusion and the rotational motion of dipoles in dielectric relaxation, as a consequence of the dynamic heterogeneity [11–14]. Therefore, this decoupling modifies the SED relationship and the equality of the rotational and translational viscosities.

Furthermore, taking into account Eq. (4), the relationship between the modulus and phase angle of the rotational and translational viscosities can be written as follows:

$$|\eta^*_{\mathrm{rot}}|(\omega) = B[|\eta^*_{\mathrm{trans}}|(\omega\delta)]^{\xi}, \tag{5a}$$

$$\varphi_{\mathrm{rot}}(\omega) = \xi\varphi_{\mathrm{trans}}(\omega\delta). \tag{5b}$$

These two equations are used to relate the dielectric and mechanical experimental measurements. The interconversion algorithm is applied in all frequency range.

A. Definition of rotational viscosity

The rotational viscosity was defined [10] by using the generalization of the DMB equation based on the use of a fractional Fokker-Planck equation; where a Cole-Cole-like equation is obtained as a fractional-power rotational viscosity in a natural way. Therefore, the generalized rotational viscosity $[\eta^*_{\mathrm{rot}}(\omega)]$ could be defined in terms of the following relation:

$$\frac{\varepsilon^* - \varepsilon_\infty}{\varepsilon_0 - \varepsilon_\infty} = \frac{1}{1 + [i\omega A\eta^*_{\mathrm{rot}}(\omega)]^a}, \tag{6}$$

where A is the same parameter given in Eq. (1). The parameter a might be chosen in such a way that the real and imaginary parts of the rotational viscosity show divergence. This value of a corresponds to the slope of the loss permittivity at lower frequency. The definition of rotational viscosity is according to that obtained by Nee and Zwanzig [15] based on the fluctuation-dissipation theorem with $\eta^*_{\mathrm{rot}}(\omega)$ proportional to the dielectric friction. They considered a rotational spherical molecule in a molecular environment acted on by a definite torque produced by the external electric field. In particular, Nee and Zwanzig's approach showed the nature of the rotational viscosity related to the opposition to rotation when a torque is acting on the dipole. So this frictional quantity is a microscopic one and in the macroscopic theory is given in a statistical sense; the rotational viscosity cannot be experimentally observed.

B. Definition of translational viscosity

The generalized translational viscosity can be defined using the Laplace transform of the fractional time derivative [10]. In this case, the viscoelastic definition of translational viscosity using the fractional time derivative is

$$G_s(t) - G_s(t=\infty) = K_{\mathrm{trans}}\frac{d^c\eta_{\mathrm{trans}}(t)}{dt^c}, \tag{7}$$

where K_{trans} is a constant with dimension [s^{c-1}] and is taken equal to 1 for the sake of simplicity. c is a parameter that should be chosen such that the real part of the translational viscosity does not show any divergence at lower frequency. The Laplace transform of Eq. (7) is

$$G^*_s(\omega) - G_0 = K_{\mathrm{trans}}(i\omega)^c\eta^*_{\mathrm{trans}}(\omega), \tag{8}$$

where the translational viscosity has the dimension [Pa s].

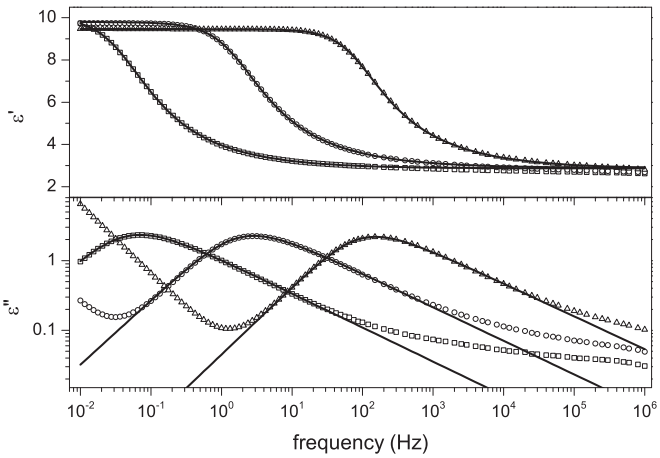

FIG. 1. Real and imaginary parts of the complex dielectric permittivity as a function of frequency at 222 K (squares), 228 K (circles), and 236 K (triangles), and fitting curves (lines).

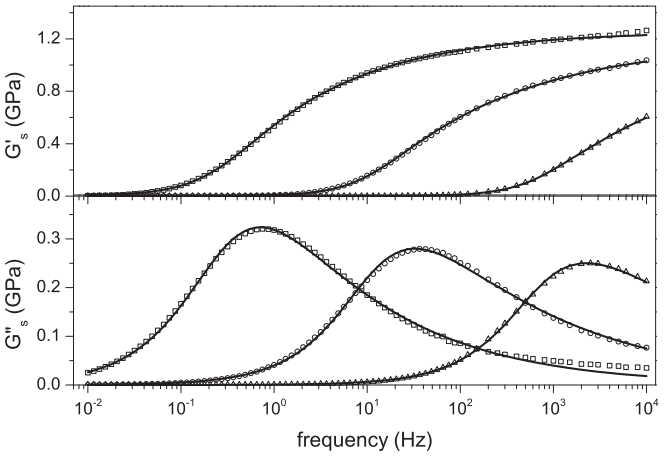

FIG. 2. Real and imaginary parts of the shear modulus as a function of frequency at 222 K (squares), 228 K (circles), and 236 K (triangles), and fitting curves (lines).

III. EXPERIMENTAL PART

The PHMD was prepared as previously reported [16]. The glass transition temperature of PHMD was measured with a TA Q-10, differential scanning calorimetry (DSC) apparatus at a heating rate of 10 K/min. Taking T_g as the temperature corresponding to the middle point of the glass-liquid endotherm of the second scan, the value of the quantity was 225 K.

The dielectric and mechanical measurements of PHMD were done at IMFUFA, Roskilde University Center, Denmark. The shear measurements were performed by using the piezoelectric shear modulus gauge (PSG) method. In the PSG method the modulus is obtained from measurements of the capacitance of the empty and the loaded gauge, a transducer based on piezoelectric plates [17]. Capacitances were measured with an HP 3458A multimeter in the range of 10^{-2} to 10^{2} Hz and an Agilent 4284A LCR meter in the range of 10^{2} to 10^{6} Hz. The temperature was controlled by a home-built nitrogen-cooled cryostat [17]. The dielectric and mechanical measurements were measured in the same cryostat. The range of temperature was from 218 to 240 K in isothermal conditions with 2 K steps.

A. Experimental results of dielectric characterization

The dielectric permittivity and loss for the PHMD are shown in Fig. 1, where the important α relaxation can be observed, secondary relaxations are present as shoulders at higher frequency, and the conductivity contribution shows in the loss permittivity at lower frequency. The conductive contribution is separated from the loss permittivity by use of a hopping model [18–20], namely,

$$\varepsilon''_{\text{cond}} = \frac{\sigma_{dc}}{\varepsilon_{\text{vac}}\omega^{s}}. \tag{9}$$

where σ_{dc} is the dc conductivity, ε_{vac} is the permittivity of the vacuum ($\varepsilon_{\text{vac}} = 8.854\,188 \times 10^{-12}$ F/m) and ω is the angular frequency. The s exponents of PHMD are close to unity for all temperatures analyzed.

The α relaxation without the conductive contribution was analyzed via the HN equation [21]:

$$\varepsilon^{*}(\omega) = \varepsilon_{\infty} + \frac{\Delta\varepsilon}{[1 + (i\omega\tau_D)^{a_{HN}}]^{b}}, \tag{10}$$

where ε_{∞} is the unrelaxed permittivity, $\Delta\varepsilon = \varepsilon_0 - \varepsilon_{\infty}$ is the strength of the relaxation, ε_0 is the relaxed permittivity, a_{HN} and b are two parameters related to the shape and skewness of the Cole-Cole plot, and τ_D is the characteristic relaxation time. The HN parameters are summarized in the Appendix. According to our fit results: (i) The unrelaxed permittivity is practically constant with temperature, with a value that is rounded to 2.86 ± 0.03. (ii) The relaxation strength decreases with the temperature, as is characteristic of α relaxations. The values of the strength of the relaxation vary between 7.47 for 218 K and 6.49 for 240 K. (iii) The parameters a_{HN} and b are nearly constant with temperature. The a_{HN} parameter is close to 1, 0.93 ± 0.04, and the b parameter is 0.52 ± 0.03. (iv) The variation of the characteristic relaxation time with temperature is bigger than for other parameters, from 52.1 s at 218 K to 3.75×10^{-4} s at 240 K.

B. Experimental results of mechanical characterization

The storage and loss shear moduli are shown in Fig. 2. The frequency range in this figure is from 10^{-2} to 10^{4} Hz. The storage and loss shear moduli from 10^{4} to 10^{5} Hz are not represented because the noise is bigger than the mechanical measurement. In this figure two relaxation processes can be observed: an α relaxation corresponding to the glass transition, and secondary relaxation, which appears as a shoulder at high frequency.

In order to characterize and analyze the mechanical spectra an HN-type equation was used:

$$G^{*}_{s}(\omega) = G_{\infty} - \frac{G_{\infty} - G_0}{[1 + (i\omega\tau_s)^{c_{HN}}]^{d}}, \tag{11}$$

where G_0 and G_{∞} are the relaxed and unrelaxed moduli, respectively, $G_{\infty} - G_0$ is the strength of the mechanical relaxation, c_{HN} and d are two parameters related to the shape

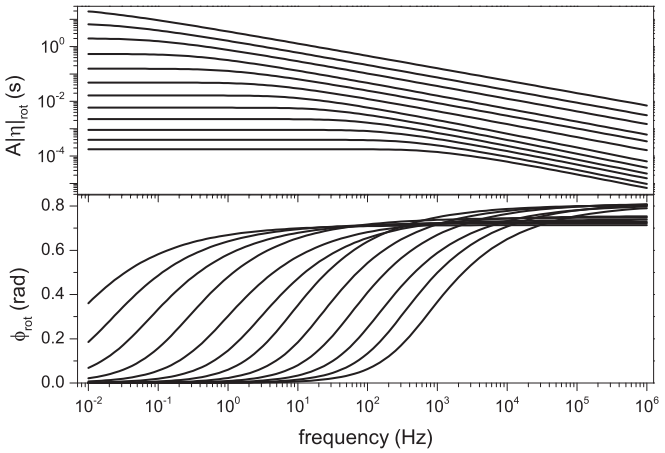

FIG. 3. Modulus and phase angle of the α rotational viscosity as a function of frequency at temperatures between 218 and 240 K (in steps of 2 K).

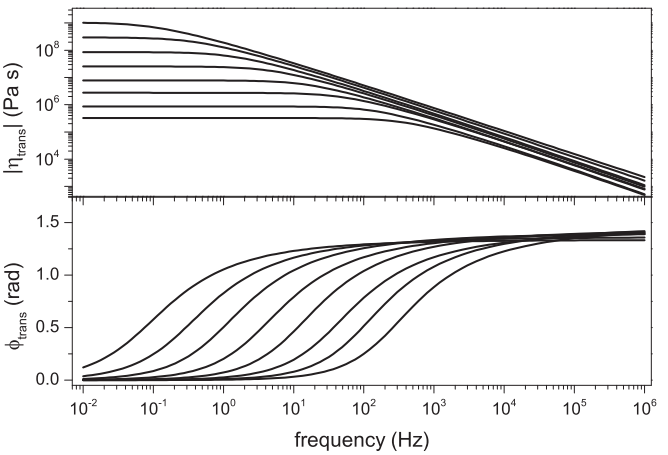

FIG. 4. Modulus and phase angle of α translational viscosity as a function of frequency at temperatures between 220 and 234 K (in steps of 2 K)

and skewness of the Argand plot, and τ_s is the characteristic relaxation time. As $G_0 \ll G_\infty$, G_0 may be neglected and $G_\infty - G_0 \approx G_\infty$. The values of the parameters from Eq. (11) are summarized in the Appendix. According to our fit results: (i) The unrelaxed modulus increases with temperature from 1.16 GPa (220 K) to 1.30 GPa (238 K). (ii) The c_{HN} and d parameters are nearly constant with temperature, with values of 0.89 ± 0.04 and 0.34 ± 0.09, respectively. (iii) The variation of the mechanical characteristic relaxation time is from 2.15 s (220 K) to 9.56×10^{-5} s (238 K).

IV. RELATION BETWEEN VISCOSITIES: THE INTERCONVERSION ALGORITHM

The procedure for establishing the interconversion was to consider the modulus and phase angle of the complex viscosities. The interconversion algorithm applied to PHMD and the interconversion parameters were determined. The rotational modulus was defined and characterized by an HN-type equation. Finally, the interconversion algorithm was defined in terms of rotational and shear moduli.

A. Determination of the rotational viscosity

In our approach, the rotational viscosity can be expressed in terms of the dielectric permittivity [see Eq. (6)]. The parameter a should be chosen by fitting, in such a way that the real and imaginary parts of the rotational modulus do not show any divergence. The parameter a is the slope of the loss permittivity and coincides with the a_{HN} shape parameter in the HN equation [Eq. (9)] ($a = a_{HN}$), because of the requirement for consistency at the low-frequency limit. The rotational viscosity can be expressed in terms of HN parameters by a combination of Eqs. (6) and (10), namely,

$$A\eta^*_{\rm rot}(\omega) = \frac{1}{i\omega}\{[1 + (i\omega\tau_D)^a]^b - 1\}^{1/a}. \qquad (12)$$

The modulus and phase angle of rotational viscosity are shown in Fig. 3. The modulus of rotational viscosity is constant at lower frequencies until a turning point is reached whereit linearly decreases on a logarithmic scale. The rotational phase angle is zero at lower frequency, presents an inflection point, and eventually grows to a constant value(0.7 ± 0.1 rad)

The frequency of the inflection point increases with the temperature.

B. Determination of the translational viscosity

The translational viscosity can be expressed in terms of HN parameters by a combination of Eqs. (8) and (11):

$$\eta^*_{\rm trans}(\omega) = \frac{1}{(i\omega)^c}\left(G_\infty - \frac{G_\infty}{[1 + (i\omega\tau_s)^c]^d}\right). \qquad (13)$$

Note that $K_{\rm trans}$ in Eq. (8) is taken equal to 1 for the sake of simplicity and the $G_\infty - G_0 \approx G_\infty$ approximation was used. The parameter c should be chosen by fitting in such a way that the real and imaginary parts of the translational modulus do not show any divergence. Note that c and c_{HN} are the same parameter ($c = c_{HN}$), because of the requirement for consistency at the low-frequency limit.

The evaluated modulus and phase angle of translational viscosity from Eq. (13) are given in Fig. 4. The form of the translational viscosity is very similar to that of the rotational viscosity. The modulus of the translational viscosity is constant at lower frequency until a turning pointis reached. The plateau of the modulus of translational viscosity decreases with temperature, whereas the turning point increases with temperature. The modulus of the translational viscosity linearly decreases on a logarithmic scale at higher frequency. On the other hand, the translational phase angle is zero at lower frequency until an inflection point, where it increases to a constant value (1.1–1.4 rad). At this point, it is convenient to emphasize that the slope of the modulus of viscosity at a higher frequency and the turning point are different for rotational and translational viscosity.

C. Interconversion algorithm for the relationship between the two viscosities

A special case of Eq. (4) is the static situation, where the dynamic viscosities become static. In this case, the shift factor

is eliminated; the interconversion algorithm becomes

$$\eta_{\rm rot}(0) = B\eta_{\rm trans}(0)^{\xi} \tag{14}$$

and only two parameters are necessary to relate the static viscosities. This expression corresponds to the FSED relation [22], where the moduli of the viscosities are exponential, decreasing at a higher frequency, and can be expressed by means of the following equations:

$$|\eta^*_{\rm rot}|(\omega) = B_{\rm rot}\omega^{-n_{\rm rot}} \tag{15}$$

and

$$|\eta^*_{\rm trans}|(\omega) = B_{\rm trans}\omega^{-n_{\rm trans}}. \tag{16}$$

The interconversion algorithm at higher frequency can be expressed in the following way, according to Eq. (5a):

$$B_{\rm rot}\omega^{-n_{\rm rot}} = B[B_{\rm trans}(\omega\delta)^{-n_{\rm trans}}]^{\xi}, \tag{17}$$

that is, $B\frac{B^{\xi}_{\rm trans}}{B_{\rm rot}}\delta^{(-\xi n_{\rm trans})}\omega^{(n_{\rm rot}-\xi n_{\rm trans})} = 1$, and consequently $n_{\rm rot} - \xi n_{\rm trans} = 0$

The exponential factor ξ can be determined via the expression

$$\xi = \frac{n_{\rm rot}}{n_{\rm trans}} \tag{18}$$

and the preexponential parameter B via

$$B = \frac{B_{\rm rot}}{B^{n_{\rm rot}/n_{\rm trans}}_{\rm trans}}\delta^{n_{\rm rot}}. \tag{19}$$

The preexponential factor B, by a combination of Eqs. (14) and (18), can also be expressed in term of static viscosities as follows:

$$B = \frac{\eta_{\rm rot}(0)}{\eta_{\rm trans}(0)^{\xi}} = \frac{\eta_{\rm rot}(0)}{\eta_{\rm trans}(0)^{n_{\rm rot}/n_{\rm trans}}}. \tag{20}$$

Furthermore, the shift factor can be expressed by a combination of Eqs. (19) and (20),

$$\delta = \left(\frac{\eta_{\rm rot}(0)}{B_{\rm rot}}\right)^{1/n_{\rm rot}}\left(\frac{B_{\rm trans}}{\eta_{\rm trans}(0)}\right)^{1/n_{\rm trans}}. \tag{21}$$

The interconversion parameters determined using Eqs. (18), (20), and (21) are summarized in the Appendix. The scale factor B increases with temperature from 5.15×10^{-5} Pa$^{\xi}$ s$^{1-\xi}$ (222 K) to 8.77×10^{-7} Pa$^{\xi}$ s$^{1-\xi}$ (236 K). The shape factor ξ is constant with temperature at around 0.56 ± 0.02, and the shift factor δ increases with temperature from 4.17 (222 K) to 5.37 (236 K). The interconversion parameters can be determined from the parameters that characterize the form of the rotational and translational viscosities.

The correspondence of the interconversion model can be observed in Fig. 5, where three isotherms are compared. The parameters of the interconversion model are summarized in the Appendix.

D. Alternative interconversion algorithm using rotational and shear moduli

The rotational modulus from rotational viscosity can be defined by means of the fractional [23] time derivative for non-Newtonian behavior as follows:

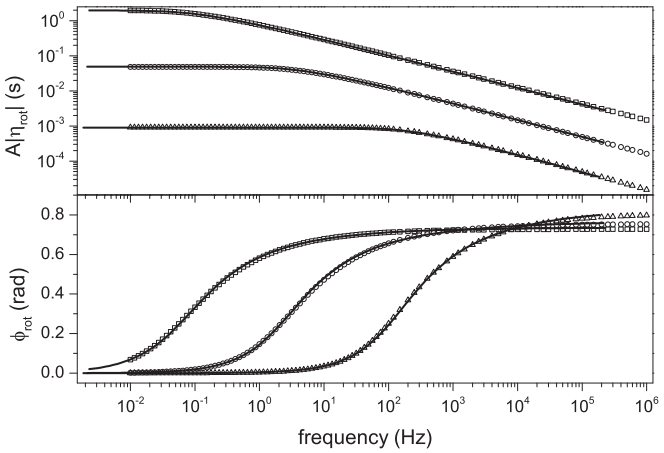

FIG. 5. Comparison of modulus and phase angle of α rotational viscosity determined from dielectric measurements Eq. (12) [222 K (square), 228K (circle), 236 K (triangle)] and from mechanical measurements using interconversion model Eq. (4) (lines).

$$G_{\rm rot}(t) - G_{\rm rot}(t=\infty) = K_{\rm rot}\frac{d^n\eta_{\rm rot}(t)}{dt^n}. \tag{22}$$

By taking the Laplace transform of this equation, the rotational modulus can be expressed by

$$G^*_{\rm rot}(\omega) - G_{\rm rot}(0) = K_{\rm rot}(i\omega)^n\eta^*_{\rm rot}(\omega), \tag{23}$$

where $K_{\rm rot}$ is a constant with dimension [s^{n-1}], and is set equal to 1 for the sake of simplicity. n is a parameter that should be chosen in such a way that the real and imaginary parts of the rotational modulus do not show any divergence. As for the case of translation viscosity, the value of n is the HN shape parameter for the rotational modulus, that is, $n = e$ [see Eq. (26)]. The rotational modulus has the dimension [Pa], as a typical modulus:

$$G^*_{\rm rot}(\omega) - G_{\rm rot}(0) = (i\omega)^e\eta^*_{\rm rot}(\omega). \tag{24}$$

The rotational modulus can be expressed in terms of HN parameters by a combination of Eqs. (12) and (24). The rotational modulus is shown in Fig. 6. The product of A and $G_{\rm rot}$ is dimensionless:

$$A[G^*_{\rm rot}(\omega) - G_{\rm rot}(0)] = (i\omega)^{e-1}\{[1+(i\omega\tau_D)^a]^b - 1\}^{1/a}. \tag{25}$$

The rotational modulus can be expressed by a mechanical HN-type equation, which has also been characterized using the shear modulus:

$$A[G^*_{\rm rot}(\omega) - G_{\rm rot}(0)] = A[G_{\rm rot}(\infty) - G_{\rm rot}(0)] - \frac{A[G_{\rm rot}(\infty) - G_{\rm rot}(0)]}{\left[1+\left(i\omega\tau_{G_{\rm rot}}\right)^e\right]^f}, \tag{26}$$

where $G_{\rm rot}(0)$ and $G_{\rm rot}(\infty)$ are the relaxed and unrelaxed moduli, respectively, $\Delta G_{\rm rot} = G_{\rm rot}(\infty) - G_{\rm rot}(0)$ is the strength of the rotational modulus, e and f are two parameters related to the shape and skewness of the Argand plot, and $\tau_{G_{\rm rot}}$ is the characteristic time. According to our results, (i) the product of A and the strength of the rotational

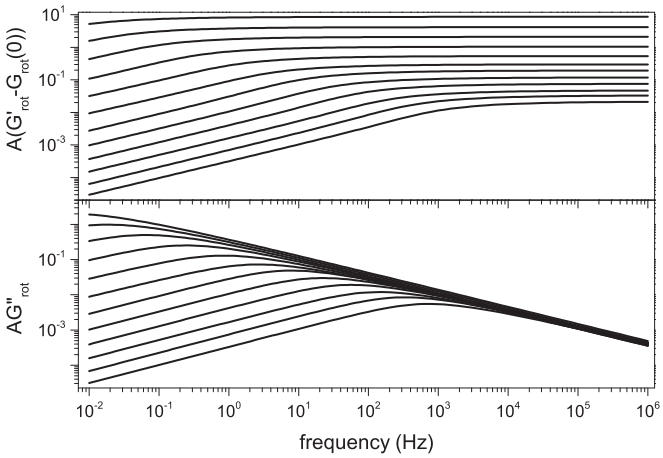

FIG. 6. Real and imaginary parts of the rotational modulus as a function of frequency at temperatures between 218 and 240 K (in steps of 2 K).

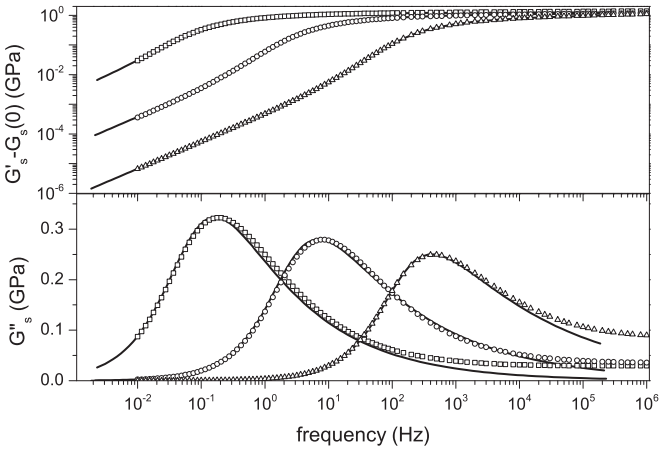

FIG. 7. Comparison between the shear modulus determined from rotational modulus (line) and shear modulus at 222 K (squares), 228 K (circles), and 236 K (triangles).

modulus, $A[G_{\rm rot}(\infty) - G_{\rm rot}(0)]$, increases with temperature from 2.10 (222 K) to 2.15×10^{-2} (240 K). (ii) The shape and skewness parameters are constant with temperature at around $e = 0.60 \pm 0.02$ and $f = 0.86 \pm 0.03$. (iii) The characteristic time decreases with temperature from 3.38 s (222 K) to 2.37×10^{-4} s (240 K). The values of the fit parameters from Eq. (26) are summarized in the Appendix.

The interconversion algorithm can be expressed in terms of the moduli by a combination of Eqs. (4), (8), and (24):

$$A[G^*_{\rm rot}(\omega) - G_{\rm rot}(0)] = \frac{AB K_{\rm rot}}{\delta^{c\xi} K^{\xi}_{\rm trans}} (i\omega)^{(e-c\xi)} [G^*_s(\omega\delta) - G_s(0)]^{\xi}. \quad (27)$$

Note that the term with the exponential of $i\omega$ diverges to infinity when the exponent is positive, and tends to zero when the exponent is negative. The rotational modulus cannot diverge to infinity or tend to zero at infinite frequency. Then $(i\omega)^{(e-c\xi)}$ must be 1, and consequently the exponent is zero, $e - c\xi = 0$, which can be numerically verified (see the Appendix). Therefore, the interconversion algorithm in terms of the moduli is

$$A[G^*_{\rm rot}(\omega) - G_{\rm rot}(0)] = M[G^*_s(\omega\delta) - G_s(0)]^{\xi}. \quad (28)$$

where $M = AB K_{\rm rot}/\delta^{c\xi} K^{\xi}_{\rm trans}$ is a scale factor.

The relationship between rotational and shear moduli is similar to the relationship between the rotational and translational viscosities.

In order to check Eq. (28), we determine that the shear modulus was obtained by dielectric measurement, and this modulus was compared with the shear modulus. The M scale factor is calculated by a simple horizontal shift of the real and imaginary parts of the rotational modulus. The values of the real and imaginary shear modulis evaluated from dielectric data and obtained from experimental mechanical measurements are very similar, as can be seen in Fig. 7.

V. SUMMARY AND CONCLUSIONS

The dielectric and mechanical characterization of PHMD were obtained by special equipment for consecutive measurements. This substance is an interesting glass-forming liquid, since the α relaxation is very dominant compared to secondary relaxations that allow data parametrization using the HN equation.

The comparison between dielectric and mechanical measurements for α relaxation of PHMD has been carried out by means of an algorithm reported elsewhere [10], by using a relation between rotational and translational complex viscosities. In particular, this relation has three parameters that are related to a scale factor (B), a shape factor (ξ), and a horizontal shift (δ). The scale factor corresponds to different magnitudes of dielectric and mechanical measurements. The shape factor is an exponent that takes into account the kinetic differences of the two viscosities. The horizontal shift is indicative of a delay time between molecular rotational and translational motions (they are out of phase).

The most valuable physical interpretation lies in the structure factor (ξ), since it represents the breakdown of the SED relation. In addition, the physical interpretation of this parameter is the decoupling of rotational and translation molecular motions. When the shape factor is equal to 1, it represents that the two motions are totally coupled or they produce the same result in each viscosity. On the other hand, when the shape factor is equal to zero it indicates that the motions are totally decoupled, they are independent of each other, and in the present algorithm there is no interconversion between them, as is the case for β relaxation.

For PHMD, the shape factor is independent of temperature, and is about 0.54 ± 0.02, and the rotational and translation molecular motions are partially decoupled. This effect can be explained by dynamical heterogeneity. In fact, there are different dynamical heterogeneities for the translational andf rotational motions, which produces multiple relaxation times involving groups of molecules with different mobilities, slower or faster [24]. The superposition of the two heterogeneities causes the breakdown of the SED relation. In the present

algorithm, this factor is expressed as a ratio of the exponents of the frequency dependence of the modulus of each viscosity in the wing of high frequencies, as is given in Eq. (18). According to our results, the shape factor also can be given by $\xi = e/c$, where e and c are the fractional exponent of $i\omega$ in the relationship of the complex viscosity and the electric and mechanical complex modulus, respectively. Thus, the breakdown of the SED is associated with the nonlinear viscoelastic relationship as is given in Eqs. (8) and (24).

Finally, an alternative interconversion algorithm was established in this paper, using dielectric and mechanical moduli. In fact, starting from the relationship of the viscosities, a relation between the shear modulus and the electric or rotational modulus was obtained.

The interconversion algorithm as proposed here, for dielectric and mechanical measurements, has a high compatibility between estimated results and the experimental data in a broad interval of frequency.

ACKNOWLEDGMENTS

The authors thank Professor Niels Boye Olsen and Jeppe C. Dyre from Roskilde Universitetcenter (Denmark) for dielectric and mechanical measurements. This work was supported by DGAPA-UNAM Projects No. IG-100315, SEP-CONACYT 154626, M.J.S. gratefully acknowledge the CICYT for grant MAT2012-3383.

APPENDIX

1. Havriliak-Negami empirical model for dielectric α relaxation of PHMD:

The Havriliak-Negami empirical model is given by for dielectric α relaxation is given by

$$\varepsilon^*(\omega) = \varepsilon_\infty + \frac{\Delta\varepsilon}{[1 + (i\omega\tau_D)^a]^b},$$

where ε_∞ is the unrelaxed permittivity, $\Delta\varepsilon = \varepsilon_0 - \varepsilon_\infty$ is the strength of the relaxation, ε_0 is the relaxed permittivity, a and b are two parameters related to the shape and skewness of the Argand plot, and τ_D is the characteristic relaxation time.

Fit parameters of HN model for dielectric α relaxation of PHMD.

T (K)	ε_∞	$\Delta\varepsilon$	a	b	τ_D (s)
218	2.82	7.47	0.89	0.55	5.21×10^{1}
220	2.84	7.35	0.90	0.54	1.41×10^{1}
222	2.86	7.21	0.91	0.54	4.01×10^{0}
224	2.87	7.09	0.92	0.52	1.09×10^{0}
226	2.89	7.01	0.92	0.53	3.14×10^{-1}
228	2.89	6.91	0.93	0.52	9.89×10^{-2}
230	2.86	6.82	0.96	0.49	3.48×10^{-2}
232	2.86	6.75	0.96	0.48	1.25×10^{-2}
234	2.85	6.68	0.97	0.48	4.78×10^{-3}
236	2.85	6.61	0.97	0.49	1.92×10^{-3}
238	2.83	6.56	0.97	0.48	8.38×10^{-4}
240	2.83	6.49	0.97	0.49	3.75×10^{-4}

2. Havriliak-Negami empirical model for shear modulus α relaxation of PHMD

The Havriliak-Negami empirical model for shear modulus α relaxation is given by

$$G_s^*(\omega) = G_\infty - \frac{G_\infty - G_0}{[1 + (i\omega\tau_s)^c]^d},$$

where G_0 and G_∞ are the relaxed and unrelaxed moduli, respectively, $G_\infty - G_0$ is the strength of the mechanical relaxation, c and d are two parameters related to the shape and skewness of the Argand plot, and τ_s is the characteristic relaxation time. As $G_0 \ll G_\infty$, G_0 may be neglected and $G_\infty - G_0 \approx G_\infty$.

Fit parameters for Havriliak-Negami for shear modulus α relaxation of PHMD.

T (K)	G_∞ (GPa)	c	d	τ_s (s)
220	1.16	0.85	0.43	2.15×10^{0}
222	1.16	0.87	0.39	5.58×10^{-1}
224	1.20	0.89	0.34	1.68×10^{-1}
226	1.19	0.89	0.33	4.66×10^{-2}
228	1.16	0.91	0.31	1.45×10^{-2}
230	1.19	0.90	0.31	4.54×10^{-3}
232	1.22	0.93	0.27	1.75×10^{-3}
234	1.26	0.93	0.25	6.56×10^{-4}
236	1.26	0.92	0.26	2.40×10^{-4}
238	1.30	0.92	0.26	9.56×10^{-5}

3. Interconversion model for PHMD

The interconversion model for PHMD is given by

$$\eta^*_{\text{rot}}(\omega) = B[\eta^*_{\text{trans}}(\omega\delta)]^\xi,$$

where B is a scale factor, ξ is a form factor, and δ is a shift factor.

Parameters of interconversion model for PHMD.

T (K)	B ($\text{Pa}^\xi\ \text{s}^{1-\xi}$)	ξ	δ
222	5.15×10^{-5}	0.54	4.17
224	2.80×10^{-5}	0.54	4.51
226	1.79×10^{-5}	0.53	4.63
228	9.48×10^{-6}	0.54	4.68
230	2.94×10^{-6}	0.58	5.22
232	2.34×10^{-6}	0.57	4.96
234	1.45×10^{-6}	0.58	5.08
236	8.77×10^{-7}	0.58	5.37

4. Moduli of the rotational and translational viscosities for PHMD

The moduli of the rotational and translational viscosities for PHMD are given by

$$|\eta^*_{\text{rot}}|(\omega) = B_{\text{rot}}\omega^{-n_{\text{rot}}},$$
$$|\eta^*_{\text{trans}}|(\omega) = B_{\text{trans}}\omega^{-n_{\text{trans}}},$$

where n_i is the slope and B_i are the preexponent factors of the modulus of the viscosity ($i = rot$ or $trans$).

Static viscosity, slope and pre-exponent factors for rotational and translational viscosities at higher frequency.

T (K)	$\eta_{\rm rot}(0)$ (Pas)	$n_{\rm rot}$	$B_{\rm rot}$	$\eta_{\rm trans}(0)$ (Pas)	$n_{\rm trans}$	$B_{\rm trans}$
222	1,99	0.46	8.39×10^{-1}	2.96×10^{8}	0.84	2.01×10^{8}
224	5.42×10^{-1}	0.47	3.98×10^{-1}	8.61×10^{7}	0.86	1.79×10^{8}
226	1.57×10^{-1}	0.46	2.05×10^{-1}	2.55×10^{7}	0.87	1.59×10^{8}
228	4.88×10^{-2}	0.47	1.11×10^{-1}	7.83×10^{6}	0.87	1.38×10^{8}
230	1.64×10^{-2}	0.50	6.56×10^{-2}	2.75×10^{6}	0.86	1.23×10^{8}
232	5.88×10^{-3}	0.50	3.91×10^{-2}	8.67×10^{5}	0.88	9.65×10^{7}
234	2.25×10^{-3}	0.50	2.39×10^{-2}	3.25×10^{5}	0.87	7.88×10^{7}
236	9.09×10^{-3}	0.50	1.45×10^{-2}	1.44×10^{5}	0.85	6.83×10^{7}

5. HN model for α relaxation of the rotational modulus of PHMD

The HN model for the α relaxation of the rotational modulus of PHMD is

$$A[G^*_{\rm rot}(\omega) - G_{\rm rot}(0)] = A[G_{\rm rot}(\infty) - G_{\rm rot}(0)] - \frac{A[G_{\rm rot}(\infty) - G_{\rm rot}(0)]}{\left[1 + \left(i\omega\tau_{G_{\rm rot}}\right)^e\right]^f},$$

where $G_{\rm rot}(0)$ and $G_{\rm rot}(\infty)$ are the relaxed and unrelaxed moduli, respectively, $\Delta G_{\rm rot} = G_{\rm rot}(\infty) - G_{\rm rot}(0)$ is the strength of the rotational modulus, e and f are two parameters related to the shape and skewness of the Argand plot, and $\tau_{G_{\rm rot}}$ is the characteristic time.

Parameters of HN equation for rotational modulus for PHMD.

T (K)	$A \times \Delta G_{\rm rot}$	e	f	$\tau_{\rm Grot}$ (s)
222	2.10×10^{0}	0.59	0.83	3.38×10^{0}
224	1.05×10^{0}	0.59	0.86	8.34×10^{-1}
226	5.40×10^{-1}	0.57	0.90	2.15×10^{-1}
228	2.99×10^{-1}	0.58	0.90	6.59×10^{-2}
230	1.94×10^{-1}	0.61	0.83	2.49×10^{-2}
232	1.19×10^{-1}	0.61	0.83	8.75×10^{-3}
234	7.56×10^{-2}	0.62	0.84	3.30×10^{-3}
236	4.71×10^{-2}	0.61	0.87	1.26×10^{-3}
238	3.32×10^{-2}	0.62	0.85	5.56×10^{-4}
240	2.15×10^{-2}	0.61	0.89	2.37×10^{-4}

6. Scale factor for the interconversion of rotational and shear moduli

The scale factor for the interconversion of rotational and shear moduli is given by

$$A[G^*_{\rm rot}(\omega) - G_{\rm rot}(0)] = M[G^*_s(\omega\delta) - G_s(0)]^{\xi},$$

where M is the scale factor ($M = ABK_{\rm rot}/\delta^{c\xi}K^{\xi}_{\rm trans}$).

M scale factor.

T (K)	M (Pa$^{-\xi}$)	T (K)	M (Pa$^{-\xi}$)
222	2.4×10^{-5}	230	1.1×10^{-6}
224	1.3×10^{-5}	232	8.5×10^{-7}
226	8.6×10^{-6}	234	4.9×10^{-7}
228	4.1×10^{-6}	236	2.8×10^{-7}

[1] A. Germant, Trans. Faraday Soc. **31**, 1582 (1935).
[2] E. A. Dimarzio and M. Bishop, J. Chem. Phys. **60**, 3802 (1974).
[3] R. Byron Bird and A. Jeffrey, Giacomin. Rheol. Acta **51**, 481 (2012).
[4] R. Díaz-Calleja, E. Riande, and J. San Román, J. Polym. Sci. Polym. Phys. **31**, 711 (1993).
[5] E. Fatuzzo and P. R. Mason. Proc. Phys. Soc. (London) **90**, 729 (1967).
[6] R. Zorn, F. I. Mopsik, G. B. McKenna, L. Willner, and D. Richter. J. Chem. Phys. **107**, 3645 (1997).
[7] D. Ferri and L. Castellani, Macromolecules **34**, 3973 (2001).
[8] K. Niss, B. Jakobsen, and N. B. Olsen, J. Chem. Phys. **123**, 234510 (2005).
[9] T. Christensen and N. B. Olsen, J. Non-Cryst. Solids **172**, 357 (1994).
[10] A. Garcia-Bernabé, M. J. Sanchis, R. Díaz-Calleja, and L. F. del Castillo, J. Appl. Phys. **106**, 014912 (2009).
[11] H. Sillescu, J. Non-Cryst Solids **243**, 81 (1999).
[12] S. R. Becker, P. H. Poole, and F. W. Starr, Phys. Rev. Lett. **97**, 055901 (2006).
[13] F. Fujara, B. Geil, H. Sillescu, and G. Fleischer, Z. Phys. B: Condens Matter **88**, 195 (1992).
[14] S. C. Glotzer, V. N. Novikov, and T. B. Schoder, J. Chem. Phys. **112**, 509 (2000).
[15] T. W. Nee and R. Zwanzig, J. Chem. Phys. **52**, 6353 (1970).
[16] E. Saiz, E. Riande, R. Díaz-Calleja, and J. Guzman, J. Phys Chem. **101**, 10949 (1997).
[17] T. Christensen and N. B. Olsen, Rev. Sci. Instrum. **66**, 5019 (1995).
[18] R. Coelho, Rev. Phys. Appl. **18**, 137 (1983).
[19] T. S. Sorensen, J. Colloid Interface Sci. **168**, 437 (1994).
[20] J. C. Dyre, J. Appl. Phys. **64**, 2456 (1988).
[21] S. Havriliak and S. Negami, Polymer **8**, 161 (1967).
[22] J. F. Douglas and D. Leporini. J. Non-Cryst. Solids **235–237**, 137 (1998).
[23] Nicole Heymans, Nonlin. Dyn. **38**, 221 (2004).
[24] M. G. Mazza, N. Giovambattista, H. E. Stanley, and F. W. Starr, Phys. Rev. E **76**, 031203 (2007).